The Cryosphere Discuss., 9, 6153–6185, 2015
www.the-cryosphere-discuss.net/9/6153/2015/
doi:10.5194/tcd-9-6153-2015

The Cryosphere Discussions
Open Access

Strong ELA increase causes fast mass loss of glaciers in central Spitsbergen

J. Małecki

Cryosphere Research Department, Adam Mickiewicz University, Poznań, Poland

Received: 25 September 2015 – Accepted: 9 October 2015 – Published: 6 November 2015

Correspondence to: J. Małecki (malecki.jk@gmail.com)

Published by Copernicus Publications on behalf of the European Geosciences Union.

Abstract

Svalbard is a heavily glacier covered archipelago in the Arctic. Its central regions, including Dickson Land (DL), are occupied by small alpine glaciers, which post-Little Ice Age (LIA) changes remain only sporadically investigated. This study presents a comprehensive analysis of glacier changes in DL based on inventories compiled from topographic maps and digital elevation models (DEMs) for LIA, 1960's, 1990 and 2009/11. The 37.9 ± 12.1 % glacier area decrease in DL (i.e. from 334.1 ± 38.4 km^2 during LIA to 207.4 ± 4.6 km^2 in 2009/11) has been primarily caused by accelerating termini retreat. The mean 1990–2009/11 geodetic mass balance of glaciers was −0.70 ± 0.06 $m\,a^{-1}$ (−0.63 ± 0.05 $m\,w.e.\,a^{-1}$), being one of the most negative from Svalbard regional means known from the literature. If the same figure was to be applied for other similar regions of central Spitsbergen, that would result in a considerable contribution to total Svalbard mass balance despite negligible proportion to total glacier area. Glacier changes in Dickson Land were linked to dramatic equilibrium line altitude (ELA) shift, which in the period 1990–2009/11 has been located ca. 500 m higher than required for steady-state. The mass balance of central Spitsbergen glaciers seems to be therefore more sensitive to climate change than previously thought.

1 Introduction

Small glaciers are natural indicators of climate, as they record even its slight oscillations by change of their thickness, length and area (Oerlemans, 2005). 20th century climate warming caused volume loss of ice masses on a global scale (IPCC 2013), contributing to recent rates of sea-level rise (SLR) in about a half. Despite relatively small area of glaciers and ice caps, their fresh-water input to SLR is of similar magnitude as from the largest ice-masses in the world: Antarctic and Greenland ice sheets (Radić and Hock, 2011; Gardner et al., 2013). Therefore it is of great importance to study volume changes of all glaciers on both hemispheres.

TCD
9, 6153–6185, 2015

The archipelago of Svalbard is one of the most significant arctic repositories of terrestrial ice. Glaciers cover 57 % of the islands with 34×10^3 km^2 and have a total volume of 7×10^3 km^3 (Nuth et al., 2013; Martín-Españyol et al., 2015). It is located in close proximity to warm West Spitsbergen Current and its cryosphere is hence considered as very sensitive to changing climatic and oceanic conditions (Hagen et al., 2003). Climate record suggests a sharp, early 20th century air temperature increase in Svalbard terminating the Little Ice Age period (LIA) around 1920's (Hagen et al., 2003). Cooler period between 1940's and 1960's was followed by a strongly positive summer temperature trend, being ca. 0.5 °C decade^{-1} for the period 1981–2011 (Førland et al., 2011; Nordli et al., 2014). Climate warming has led to volume loss of Svalbard glaciers, particularly after 1990 (Hagen et al., 2003; Kohler et al., 2007; Sobota, 2007; Nuth et al., 2007, 2010, 2013; Moholdt et al., 2010; James et al., 2012).

Coastal zones of Svalbard receive the highest precipitation and experience low summer temperature, hence are heavily glacier-covered. In contrast, interior of Spitsbergen, the largest island of the archipelago, shows little ice area because distance from the open seas limits moisture transport with simultaneous increase in air temperature during summer months (Hagen et al., 1993; Nuth et al., 2013; Przybylak et al., 2014). Response of glaciers to climate change in these districts has been studied much more seldom, probably because of their presupposed low significance in the overall Svalbard glacier mass balance.

One of the regions situated the furthest from maritime influences (ca. 100 km) is Dickson Land (DL). This paper inventorizes all ice masses of DL and quantifies changes of their geometry since the Little Ice Age (LIA). This includes changes of their area and length, as well as recent volume fluctuations using aerial photogrammetry. The aim of this study is to investigate recent mass balance of an inner-fjord region in central Spitsbergen and to estimate contribution of similar regions to total Svalbard mass balance.

TCD
9, 6153–6185, 2015

2 Study area

The study region is located in central Spitsbergen and stretches between 78°27′–79°10′ N and 15°16′–17°7′ E. Its area is 1.48×10^3 km^2 with length of ca. 80 km in north–south direction and typical width of 20–30 km. For the purpose of the glaciological analysis DL was divided into three subregions – south (DL-S), central (DL-C) and north (DL-N) (Fig. 1). DL-S is the lowest elevated and dominated by plateau-type mountains, with summits reaching 500–600 m a.s.l., occupied by small icefields and ice-masses plastered along gentle slopes. DL-C is the subregion with the greatest ice-cover and the largest glaciers, mostly of valley type, and summits exceeding 1000 m. The mountains in DL-N are even slightly higher than in the central part, but glaciers (mainly of valley and niche types) are smaller here and mostly oriented towards the north.

Climate of DL shows strong inner-fjord, quasi-continental characteristics, i.e. reduced precipitation and increased summer air temperature when compared to coastal regions. The southernmost inlet of DL is located about 20 km north from Svalbard Lufthavn weather station (SVL, 15 m a.s.l.) near Longyearbyen town. Between 1981 and 2010 Norwegian Meteorological Institute measured at SVL average annual temperature of −5.1 °C, with summer (June–August) mean of 4.9 °C, being relatively high as for Svalbard. Annual measured precipitation was 188 mm. In DL-C daily means of sea-level air temperature are very similar as at SVL (Rachlewicz and Styszyńska, 2007; Láska et al., 2012), but over glaciers it drops relatively fast with increasing altitude (Małecki, 2013a, 2015a). No meteorological stations are operating in DL-N, but the general climatic pattern suggests it is among the driest zones in the whole Svalbard (Hagen et al., 1993).

Previous glacial research performed in DL-C focused mainly around impact of glacier retreat on landscape remodelling (e.g. Karczewski, 1989; Kostrzewski et al., 1989; Gibas et al., 2005; Rachlewicz et al., 2007; Rachlewicz, 2009a, b; Ewertowski et al., 2010, 2012; Ewertowski and Tomczyk, 2015; Evans et al., 2012; Szpikowski et al., 2014; Strzelecki et al., 2014; Pleskot, 2015). More detailed glaciological investigations were performed on Bertilbreen (e.g. Žuravlev et al., 1983; Troicki, 1988) and recently also on Svenbreen (Małecki, 2013a, 2014; 2015b). Glaciers in central and eastern part of DL-C lose their mass and retreat their fronts (Rachlewicz et al., 2007; Małecki, 2013b; Małecki et al., 2013; Ewertowski, 2014). Glaciers of DL-N and DL-S have not been studied yet.

Glaciers of DL are mostly very small hence their dynamics are low. The maximum ice velocity measured on largest ice masses of the region did not exceed $12\,\mathrm{m\,a^{-1}}$ (Rachlewicz, 2009a), while on smaller glaciers it is several times lower (Małecki, 2014). In every subregion however surge-type glaciers occur. Studentbreen, north-eastern outlet of Frostisen icefield, surged around 1930. Fyrisbreen surged around 1960 (Hagen et al., 1993), but its front advance was by far insufficient to reach maximum position from early 20th century (compare with map by Lid, 1928). Hørbyebreen surged probably in late 19th or early 20th century (Małecki et al., 2013). Also, visual inspection of 2009/11 aerial imagery by Norwegian Polar Institute revealed that Hoegdalsbreen/Arbobreen system, Manchesterbreen and Vasskilbreen system are characterised by deformed (looped) flow lines and/or moraines, which may indicate their past surge behaviour.

3 Data and methods

3.1 Glacier geometry data

A ready-to-use Svalbard glacier geometry product by König et al. (2013) and Nuth et al. (2013) was inspected as a potential data source for the purpose of this study. Due to large, Svalbard-wide scale of König/Nuth catalogue the precision of glacier boundaries was often insufficient to accurately reproduce subtle decadal changes of very small glaciers in DL. Therefore, glacier inventories from this paper (covering glacier extents from LIA, 1960's, 1990 and 2009/11) were created with use of data from Norwegian Polar Institute (NPI). The source of 1960's glacier geometry were 1 : 100 000 S100 series topographic maps constructed from 1 : 50 000 aerial imagery by NPI taken between 1960 and 1966. As a 1990 and 2009/11 topographic background for the analysis, 20 m digital elevation models (DEMs) by NPI were used (Norwegian Polar Institute, 2014a). They were constructed from 1 : 15 000 aerial photographs (1990) and 0.5 m resolution aerial imagery (2009/11), projected into a common datum ETRS 1989 and fit into a common cell grid. Universal co-registration procedure described by Nuth and Kääb (2011) proved proper XYZ alignment of both datasets. Data for the most recent DEM origins mainly from 2011, but eastern part of DL-C was covered with earlier 2009 aerial images.

Glacier boundaries for 1960's epoch were manually digitized as polygons in ArcGIS software from scanned and georeferenced paper maps S100 series. The LIA area of glaciers was estimated by adding area of their moraine zones to 1960's glacier outlines, but no information was available for their lateral extent in that time. 1990 and 2009/11 outlines were taken from official NPI inventories (Norwegian Polar Institute, 2014b), which proved to be accurate during direct field surveys. Confluent glaciers of comparable size separated by a medial moraine were treated as individual units, except for Ebbabreen, the largest glacier in DL, historically considered as one object. Where possible, minor tributary glaciers which eventually separated from the main stream were fixed as individual glaciers also in the earlier epochs, so area changes of a given glacier result from ice melt-out, rather than from disconnection of former tributaries. Very small episodic snow fields and elongated narrow patches connected with main glacier bodies were excluded from the inventory. Hydrological ice-divides were fixed in time and did not account for changing ice topography. Small icefields Frostisen and Jotunfonna were not further divided into glacier basins.

3.2 Calculation of glacier geometry parameters and their changes

From modern glacier boundaries and 2009/11 DEM main morphometric characteristics could be extracted. Those were area (A), length (L), mean slope (S), mean aspect

TCD
9, 6153–6185, 2015

(α), minimum, maximum, median and moraines elevation (H_{min}, H_{max}, H_{med} and H_{mor} respectively) and theoretical steady-state equilibrium line altitude (tELA), assuming an accumulation area ratio of 0.6. Area was measured for each polygon and epoch (A_{max}, A_{1960}, A_{1990}, A_{2011}, respectively for each of the analysed epochs). S, α, H_{min}, H_{max} and H_{med} were computed for each polygon for 2009/11. L was calculated for each epoch along the centrelines of 62 largest valley, niche and cirque glaciers, excluding irregular ice masses with no dominant flow direction, former minor tributary glaciers that used to share front with the main glacier in their basin and very small glaciers with $A_{max} < 0.5\,\mathrm{km}^2$. In some cases more centrelines must have been used, e.g. to measure representative L of icefields with multiple outlets. Several parameters were used as indicators of glacier fluctuations, including area changes (dA), length changes (dL), volume changes over the period 1990–2009/11 (dV) and mean elevation change for the period 1990–2009/11 (dH), all given also as annual rates (dA/dt, dL/dt, dV/dt and dH/dt respectively). All rates of glacier change indicators were computed according to the year of validity of geometry data.

To compute dV elevation change pixel grids have been first calculated for each ice mass by subtraction of 2009/11 DEM from 1990 DEM. It is an accurate method of mass change measurement over long time scales (Cox and March 2004), providing information of thickness changes over the entire glacier with no need of extrapolation the mass balance values from single reference points such as stakes used in direct glaciological method. In the resulting raster, pixels lying within the larger glacier boundaries (here 1990 area) have been averaged to obtain representative elevation change value for each 1990 glacier polygon ($\overline{\mathrm{d}h}$). dV has been then calculated using the following equation:

$$\mathrm{d}V = \overline{\mathrm{d}h} \times A_{1990} \quad (1)$$

$\mathrm{d}H$ was inferred by dividing $\mathrm{d}V$ by the average area of a glacier over the period 1990–2009/11 to account for glacier retreat.

$$\mathrm{d}H = \frac{1}{\mathrm{d}V} \times \frac{(A_{1990} + A_{2011})}{2} \quad (2)$$

Near-surface glacier density changes were not considered in this study as they were assumed to be small when compared to climatically-induced elevation changes over the study period 1990–2009/11. This assumption is more uncertain in the highest zones of glaciers, where changes in firn thickness may lead to considerable density variations. However, direct field surveys and analysis of available satellite images indicate that in late summer the highest glacier zones in DL are composed almost exclusively of glacier ice or superimposed ice and almost no firn is present. Moreover, Kohler et al. (2007) have shown a good match between geodetic and glaciologically-measured cumulative mass balance on a small NW Spitsbergen glacier, implying density changes may be neglected in geodetic balance calculations on comparatively small and retreating ice masses in Svalbard. Therefore, $\mathrm{d}H/\mathrm{d}t$ could be converted to geodetic mass balance (given in metres of water equivalent, m w.e.) by multiplication by an average ice density of 900 kg m^{-3}.

3.3 Errors

Glacier area measurements for 1960/66 epoch suffer from errors associated with general map accuracy or misinterpretations made by cartographers, e.g. due to considerable extent of winter snow cover on aerial images. To account for that, 25 m has been used as a horizontal uncertainty of glacier polygon digitalisation. Each polygon has been assigned a 25 m buffer with "–" and "+" signs. Including these buffers, new areas of DL glaciers have been computed and compared to all original polygons. Differences between new and original values have been used as an error estimate of A_{1960} for each glacier, with ±6.4 % as a region-wide total and being larger for the smaller ice masses. Since no maps are available for LIA maximum, LIA glacier area estimation is based on 1960/66 outlines and geomorphological mapping of moraine zones. Such approach assumes only frontal retreat in the period LIA-1960's, but some lateral retreat most likely took place as well. Also, moraine deposits of some glaciers could have been eroded until the aerial photogrammetry era or not formed at all. Application of a relatively large ±50 m buffer around LIA outlines resulted in total glacier area error estimate of ±11.5 % for that epoch. For 1990 and 2009/11 epochs lower buffers of ±10 and ±5 m have been used, resulting in area uncertainty estimates of ±3.4 and ±2.2 % for the whole DL region. Uncertainties of length measurement for each year were set according to the buffers described above.

To estimate error of $\overline{\mathrm{d}h}$ (ε) elevation differences between 1990 and 2009/11 DEMs over non-glacier covered terrain in the whole study region were measured. Since ice surfaces in DL are relatively poorly inclined, mountain slopes steeper than 20° were excluded from the analysis. The results have shown that elevation difference of over 70 % of pixels is within ±2 m and less than 5 % are characterized by elevation difference of more than ±5 m (Fig. 2). Mean elevation difference between the two DEMs was 0.24 m, a correction further subtracted from all obtained $\overline{\mathrm{d}h}$ values, while standard deviation, σ, was 2.68 m. Here σ is used as point elevation difference uncertainty and is further used to compute ε for individual glaciers. Elevation measurement error of snow-covered surfaces was however expected to be larger than for rocks and vegetated areas due to its lower radiometric contrast on aerial images. To account for this effect, parts of glacier surfaces extending above 550 m a.s.l. (being an approximate snowline on 1990 and 2009/11 aerial imagery) have a prescribed error characteristic of 2σ. For each glacier ε has been then calculated using Eq. (3):

$$\varepsilon = \frac{[(1-n)\times\sigma] + (n\times 2\sigma)}{\sqrt{N}} \tag{3}$$

where n is a fraction of the glacier extending above 550 m and N is the sample size. Assuming spatial autocorrelation of elevation errors on the order of 1000 m after Nuth et al. (2007) N becomes glacier size in km^2 rather than number of sample points.

Using ε and errors or glacier area measurements, uncertainties of dV and dH could be assessed with conventional error propagation methods. All errors are relatively large for the smallest ice masses and vice versa.

The 1990 DEM does not fully cover major glaciers in eastern DL-C (Ebbabreen, Ragnarbreen, Bertrambreen and Pollockbreen), which represent 16.6 % of the modern glacier area of DL, so their elevation changes for 1990–2009/11 period could not be measured directly. To estimate their 1990–2009/11 thinning rates, dH/dt typical for their tELA has been used, since this parameter proved high correlation with dH/dt (described further in the Results section). This was done by selecting ice masses with similar tELA (±25 m), among which average dH/dt and its standard deviation were computed and assigned to the glacier with no direct measurements. As an error estimate for such obtained dH/dt value, 2 standard deviations of mean dH/dt among the group of glaciers with similar tELA was used.

4 Results

4.1 Modern geometry of Dickson Land glaciers

In the most recent 2009/11 inventory 152 ice masses have been catalogued in DL, all terminating on the land and covering in total 207.4 ± 4.6 km^2 (14.0 % of the region). 110 ice masses (72 % of the population) have area < 1 km^2 and 86 of them are smaller than 0.5 km^2. Only 9 glaciers (6 %) are larger than 5 km^2. The largest glaciers are Ebbabreen (24.3 km^2), Cambridgebreen/Baliollbreen system (16.3 km^2), Hørbyebreen (15.9 km^2) and Jotunfonna (14.0 km^2). North-facing glaciers (N, NW and NE) comprise 61 % of the population, while only 16 % of ice masses have a southern aspect (S, SW and SE). The mean glacier slope is 10.7°, clearly decreasing with increasing glacier area.

DL-C is the subregion with the heaviest glacier-cover with 25.9 % (117.1 km^2), whereas it is only 7.7 % (39.3 km^2) and 9.8 % (51.0 km^2) in DL-S and DL-N respectively.

The subregions also differ significantly in their area-altitude distribution. DL-N has most of high elevated glacier area of DL and median elevation of 614 m. In DL-C glacier fronts reach the lowest elevations, while glacier hypsometry of DL-S is the most flat and contains the lowest fraction of high elevated areas. Median elevations of the two latter subregions are 520 m, giving overall median elevation of glaciers in DL of 539 m and tELA of 504 m a.s.l. Larger glaciers tend to be longer, less steep and have low elevated termini. The further north, the higher are maximum and median glacier elevations. Total volume of DL ice masses, estimated with empirical area-volume scaling parameters by Martín-Español et al. (2015), is roughly 12 km^3. Details of glacier geometry characteristics are depicted in Fig. 3.

4.2 Glacier area and length reduction

Since the termination of the LIA glaciers of DL have been continuously losing their area, in total by 37.9 ± 12.1 % (Fig. 4a; Table 1). The overall rate of area change dA/dt was $-0.49 \pm 0.66\ km^2\ a^{-1}$ in the first epoch, which decreased fourfold to $-2.01 \pm 0.85\ km^2\ a^{-1}$ after 1960 and further to $-2.23 \pm 0.48\ km^2\ a^{-1}$ after 1990 (Fig. 4a). Exclusion of known and probable surge-type glaciers, which may change their extent due to internal dynamic instabilities, gives a good insight into the climate-induced area changes in the region and confirms that increasing area loss rates are related to climate forcing rather than ice dynamics (Fig. 4b). Large error bars of dA/dt do not however give a clear picture of the ongoing trend.

In contrast to dA/dt, average length change rates dL/dt suffer from minor uncertainties. With the available temporal resolution of the data all glaciers have been continuously retreating and no single front advance was detected, although surge events of Frostisen and Fyrisbreen occurred during the first analysed period, about 1930 and 1960 respectively (Hagen et al., 1993). Extreme total dL observed in DL were −46 and −3325 m. Epochs LIA–1960's or 1960's–1990 were the periods of the fastest retreat for 22.6 % of the studied glaciers. In many of these cases bedrock topography supported short-term boost of dL/dt, e.g. due to bedrock sills dissecting thinning

TCD
9, 6153–6185, 2015

glacier snouts into active and dead ice zones (e.g. Ebbabreen, Frostisen, Svenbreen). The vast majority of glaciers (77.4 %) has been retreating at their fastest rate in the last study period 1990–2009/11.

4.3 Glacier thinning and mass balance

A strikingly negative elevation change pattern is evident from the data, also in the highest zones of glaciers all over DL (Fig. 5). Considerable zones of positive elevation change were found only on high elevated glaciers in DL-N (Kaalaasbreen, Arbobreen or mountain-top ice patch on Gavlhaugen). At the lowest altitudes (< 200 m a.s.l.) mean change rate was ca. $-2\,\mathrm{m\,a^{-1}}$, while at the average tELA (ca. 500 m a.s.l.) it was about $-0.6\,\mathrm{m\,a^{-1}}$. Positive fluctuations were observed just above 1000 m a.s.l. on average (Fig. 6a). Some glaciers have been thinning at very high rate exceeding $1\,\mathrm{m\,a^{-1}}$ (e.g. Manchesterbreen and Sophusbreen), while few small ice patches have been closer to balance (Fig. 6b). Overall, average area-weighted $\mathrm{d}H/\mathrm{d}t$ in DL was highly negative at $-0.70 \pm 0.06\,\mathrm{m\,a^{-1}}$ ($-0.63 \pm 0.05\,\mathrm{m\,w.e.\,a^{-1}}$), resulting in total mass balance of $-0.14 \pm 0.01\,\mathrm{Gt\,a^{-1}}$. Subregional values are given in Table 2 and indicate the most negative specific mass balance in DL-C and the least negative in DL-N.

4.4 Statistical analysis of glacier change controls

The main driver for $\mathrm{d}H/\mathrm{d}t$ was elevation of the bulk of glacier ice, here represented by median elevation and tELA (Fig. 7a, Table 3). In result, in the epoch 1990–2009/11 the highest elevated glaciers of DL-N have been thinning the slowest, while glaciers of DL-C, having the largest portion of low-elevated ice, had the highest glacier-wide thinning rates. $\mathrm{d}L$ was correlated with terminus altitude and glacier length, so low-elevated fronts of long glaciers have been retreating at the fastest rates. Relative $\mathrm{d}A$ was best correlated with relative $\mathrm{d}L$ (Fig. 7d), indicating it was its main control. It has also shown good correlation with glacier area (Fig. 7e), maximum elevation (Fig. 7f) and length, so large glaciers lost the smallest fraction of their maximum extent despite

TCD
9, 6153–6185, 2015

significant absolute area and length losses. In contrast to reports from many other regions of the globe (e.g. Li and Li, 2014; Fischer et al., 2015; Paul and Mölg 2014), glacier aspect shown no statistical correlation with any of glacier change parameters, what may result from summertime midnight-sun over Svalbard and more balanced insolation at slopes with north and south aspects when compared to mid-latitudes.

5 Discussion

In agreement with earlier studies from Svalbard (Kohler et al., 2007; Nuth et al., 2007, 2010; 2013; James et al., 2012), climate warming is anticipated as the main control of the observed negative glacier mass balance in DL. Air temperature at SVL station has been clearly increasing in 1920's and 1930's, as well as after 1990 (Nordli et al., 2014), what explains glacier retreat after LIA maximum and in the last study epoch respectively. However, clear post-1960 mass loss acceleration of DL glaciers may not be simply explained by increased air temperature. In the period 1960–1990 total glacier area loss rate quadrupled (though with large uncertainty) and front retreat rates doubled, despite the fact that mean multidecadal summer air temperature was very similar as in the first epoch and no decrease in winter snow accumulation over Svalbard is evident at that time (Pohjola et al., 2001; Hagen et al., 2003). In this context it seems likely that average summer air temperature is not the only driver of change of small, low-activity glaciers in DL and other factors may also play a role. Those could be for example different response times of glaciers or albedo feedbacks, which could modify glacier mass balance in a non-linear pattern, e.g. by removal of high-albedo firn from accumulation zones and hence increasing energy absorption (Kohler et al., 2007; James et al., 2012; Małecki 2013b).

Wide-spread acceleration of area and length loss rates indicates that glaciers in DL have been experiencing an increasingly negative mass balance since the termination of the LIA, in line with earlier studies. For seven glaciers in DL-C Małecki (2013b) documented mean net mass change of $-0.49\,\mathrm{m\,a^{-1}}$ in the period 1960's–1990, followed by an acceleration of mass loss rate to dH/dt = −0.78 m a^{-1} after 1990. Kohler et al. (2007) analysed dH/dt of two small land-terminating glaciers in Spitsbergen with greater temporal resolution than available for this study and concluded continuous acceleration of their thinning over the 20th century, e.g. from −0.15 m a^{-1} (1936–1962) to −0.69 m a^{-1} (2003–2005) for Midre Lovénbreen in NW Spitsbergen. James et al. (2012) documented negative dH/dt for six small land-terminating glaciers all over Svalbard since 1960's and reported post-1990 increase of mass loss rates for four of them. Their recent dH/dt ranged from −0.28 to −1.21 m a^{-1}, being similar to values observed in DL.

Almost no thickening is apparent in the highest zones of glaciers in DL, since mean zero-elevation change line has shifted from ca. 600 m in the period 1960's–1990 (Małecki, 2013b) to 1000 m a.s.l. after 1990. Despite the fact that it may not necessarily agree with the true ELA (due to ice submergence in accumulation zones), on retreating stagnant glaciers of DL the latter could be expected to be similar to zero-elevation change line. Direct GPS measurements on Svenbreen (DL-C), small glacier with maximum flow velocity of only 3 m a^{-1}, confirmed that geodetic equilibrium was nearly equal to the true ELA for the period July 2010–July 2012 (Małecki, 2013a). Therefore, the presented results indicate that the ELA of most glaciers in the study region has already raised above their highest points (typically 700–800 m a.s.l.), what will eventually lead to their complete melt-out, even if the atmospheric warming trend has stopped. As suggested by glacier geometry analysis, the average ELA should be located at ca. 500 m in order for the modern glaciers to be in steady-state.

Another consequence of dramatic ELA increase is that local surge-type glaciers may not build up towards new surges and as such could be removed from the surge-cycle under present climate conditions, as demonstrated in more detail for Hørbyebreen by Małecki et al. (2013). The only exception in DL is a small glacier Arbobreen, former tributary of Hoegdalsbreen, which seems to undergo slow high-elevation thickening at a rate up to 0.25 m a^{-1}. Thinning of glaciers will also lead to decay of temperate ice zones, which are still found beneath the largest glaciers of DL (Małecki, unpublished

TCD
9, 6153–6185, 2015

data). Consequently, it will impact their hydrology, geomorphological activity and reduce ice flow dynamics, as documented for other small glaciers in central Spitsbergen (Hodgkins et al., 1999; Lovell et al., 2015).

The trend of acceleration of glaciers' front retreat in DL over the 20th and 21st centuries is similar as on most land-terminating glaciers of Svalbard (Lankauf, 2007; Zagórski et al., 2008; James et al., 2012; Nuth et al., 2013). The associated post-LIA relative glacier area decrease in DL was high with 37.9 %, supporting previous conclusions by Ziaja (2001) and Nuth et al. (2013) that central Spitsbergen, with much smaller glaciers, loses its ice cover extent at a relatively higher rate than maritime regions of Svalbard. Area loss rates in DL have been at similar level between 1960's–1990 and 1990–2009/11, in contrast to study by Nuth et al. (2013), who concluded a clear decrease in area loss rates for entire Svalbard after 1990. On the other hand, Błaszczyk et al. (2013) concluded increasing area loss rates for tidewater glaciers in Hornsund, south Spitsbergen. Interestingly, ca. 800 km^2 of glaciers in Hornsund, often considered to be the most sensitive to climate warming, have been losing area at a similar rate as ca. 200 km^2 of small glaciers in DL (ca. 1 $km^2\,a^{-1}$ for the period LIA-2000's).

In opposition to relative area changes, specific mass balance of glaciers in central Spitsbergen has been previously considered by some researchers as relatively resistant to climate change due to much drier climate and higher hypsometry (Nuth et al., 2007). However, at -0.63 ± 0.05 m w.e. a^{-1} mean specific mass balance of glaciers in DL is among the most negative from Svalbard, which overall recent surface mass balance is estimated to range from -0.12 to -0.36 m w.e. a^{-1} (Hagen et al., 2003; Nuth et al., 2010; Moholdt et al., 2010). High mass loss rates in DL may result from several factors, but primarily from high position of true ELA when compared to their theoretical steady-state ELA (tELA). The other factors could be their low glacier area/basin area ratios, strongly influencing energy balance of their valleys, and/or stronger climate forcing than in coastal zones of Svalbard.

The three regions of central Spitsbergen, i.e. DL, Nordenskiöld Land (NL) and Bünsow Land (BL) (Fig. 1) are similar in terms of climate, topography and glaciology and their total glacier cover is ca. 800 km^2 (based on dataset by Nuth et al., 2013). Since the geodetic balance measured for DL is comparable with mass balances obtained for single glaciers in NL (e.g. Troicki, 1988; Bælum and Benn, 2011), it is justified to assume it is representative for central Spitsbergen. If the specific mass balance of −0.63 m w.e. a^{-1} was to be applied also for NL and BL, that would result in mass balance contribution from these three regions of −0.5 Gt a^{-1}. It is a considerable value when compared to Svalbard-wide surface mass balance of −4.3 Gt a^{-1} calculated by Moholdt et al. (2010). Faster mass loss rates from Svalbard were also reported, e.g. by Wouters et al. (2008) (−8.8 Gt a^{-1}) or Nuth et al. (2010) (−9.7 Gt a^{-1}, excluding Austfonna and Kvitøya ice caps). Nevertheless, the presented study points that small inner-fjord glaciers in Spitsbergen interior may have more negative specific mass balance than most regions of Svalbard. Despite their negligible contribution to the total glacier area (ca. 2 %), more concern should be put on their evolution to better estimate future glacier mass balance of the archipelago, as well as on changing functioning of their valleys under conditions of fast deglaciation.

6 Conclusions

In this study new multi-temporal inventory of glaciers in Dickson Land, central Spitsbergen, has been compiled with use of snow/ice outlines and digital elevation models released by Norwegian Polar Institute. At present the region is covered with small (up to 24 km^2) land-terminating glaciers with total volume estimated to be roughly 12 km^3. Local glaciers have been losing their extent at an accelerating rate since the Little Ice Age termination (early 20th century), from 334.1 ± 38.4 km^2 in total to 207.4 ± 4.6 km^2 in 2009/11, corresponding to an overall 37.9 ± 12.1 % decrease. Post-1990 area loss rate has been 4.5 times that in the epoch LIA-1960’s, i.e. 2.23 ± 0.48 vs. 0.49 ± 0.66 km^2 a^{-1} respectively. Front retreat of 62 test-glaciers has been accelerating

TCD
9, 6153–6185, 2015

with time, being on average $5.1 \pm 0.1\,\mathrm{m\,a^{-1}}$ in the period from the maximum to 1960's, $9.4 \pm 0.1\,\mathrm{m\,a^{-1}}$ between 1960's and 1990 and as much as $17.1 \pm 0.1\,\mathrm{m\,a^{-1}}$ in the last study epoch 1990–2009/11.

The most important finding of this study is fast glacier-wide thinning over the entire region at a mean rate of $0.70 \pm 0.06\,\mathrm{m\,a^{-1}}$ ($-0.63 \pm 0.05\,\mathrm{m\,w.e.\,a^{-1}}$). It was related to strong equilibrium line altitude increase from pre-1990 600 m to 1000 m a.s.l. after 1990. It will eventually lead to complete melt-out of the study glaciers, even if the observed climate warming was to be stopped. Application of the mean specific mass balance calculated for Dickson Land to two other regions of central Spitsbergen, very similar in terms of climate and glaciology, yields an estimate of total mass balance contribution of $-0.5\,\mathrm{Gt\,a^{-1}}$ from small glaciers in the interior of Spitsbergen, a figure which should be considered in future assessments of Svalbard mass balance. In contrast to most regions of the archipelago, Dickson Land is occupied by very small, low-activity glaciers, which adjust to new climate conditions by enhanced melting, rather than by large changes in the ice flux and calving front retreat. Hence, they provide a better, easier to interpret climate indicator than larger, mostly tidewater glaciers in more maritime zones of the archipelago.

The Supplement related to this article is available online at doi:10.5194/tcd-9-6153-2015-supplement.

Acknowledgements. The study is a contribution to DIL*ICE project (Dickson Land Ice Masses Evolution, RiS id 4894) supported by the Polish National Science Centre (grant no. N306 062940). The author deeply appreciates the open-access data policy of the Norwegian Polar Institute. Comments of J.O. Hagen on the early manuscript are also greatly acknowledged.

References

Bælum, K. and Benn, D. I.: Thermal structure and drainage system of a small valley glacier (Tellbreen, Svalbard), investigated by ground penetrating radar, The Cryosphere, 5, 139–149, doi:10.5194/tc-5-139-2011, 2011.

Błaszczyk, M., Jania, J., and Kolondra, L.: Fluctuations of tidewater glaciers in Hornsund Fjord (Southern Svalbard) since the beginning of the 20th century, Pol. Polar Res., 34, 327–352, 2013.

Cox, L. H. and March, R. S.: Comparison of geodetic and glaciological mass-balance techniques, Gulkana Glacier, Alaska, USA, J. Glaciol., 50, 363–370, 2004.

Evans, D. J. A., Strzelecki, M., Milledge, D. G., and Orton, C.: Hørbyebreen polythermal glacial system, Svalbard, Journal of Maps, 8, 146–156, 2012.

Ewertowski, M.: Recent transformations in the high-Arctic glacier landsystem, Ragnarbreen, Svalbard, Geogr. Ann. A, 93, 265–285, doi:10.1111/geoa.12049, 2014.

Ewertowski, M. and Tomczyk, A.: Quantifcation of the ice-cored moraines' short-term dynamics in the high-Arctic glaciers Ebbabreen and Ragnarbreen, Petuniabukta, Svalbard, Geomorphology, 234, 211–227, doi:10.1016/j.geomorph.2015.01.023, 2015.

Ewertowski, M., Kasprzak, L., Szuman, I., and Tomczyk, A. M.: Depositional processes within the frontal ice-cored moraine system, Ragnar glacier, Svalbard, Quaestiones Geographicae, 29, 27–36, 2010.

Ewertowski, M., Kasprzak, L., Szuman, I., and Tomczyk, A. M.:. Controlled, ice-cored moraines: sediments and geomorphology, An example from Ragnarbreen, Svalbard, Z. Geomorphol., 51, 53–74, doi:10.1127/0372-8854/2011/0049, 2012.

Fischer, M., Huss, M., and Hoelzle, M.: Surface elevation and mass changes of all Swiss glaciers 1980–2010, The Cryosphere, 9, 525–540, doi:10.5194/tc-9-525-2015, 2015.

Førland, E. J., Benestad, R., Hanssen-Bauer, I., Haugen, J. E., and Skaugen, T. E.: Temperature and precipitation development at Svalbard 1900–2100, Advances in Meteorology, 2011, 893790, doi:10.1155/2011/893790, 2011.

Gardner, A. S., Moholdt, G., Cogley, J. G., Wouters, B., Arendt, A. A., Wahr, J., Berthier, E., Hock, R., Pfeffer, W. T., Kaser, G., Ligtenberg, S. R. M., Bolch, T., Sharp, M. J., Hagen, J. O., van den Broecke, M. R., and Paul, F.: A reconciled estimate of glacier contributions to sea level rise: 2003 to 2009, Science, 340, 852–857, 2013.

TCD
9, 6153–6185, 2015

Gibas, J., Rachlewicz, G., and Szczuciński, W.: Application of DC resistivity soundings and geomorphological surveys in studies of modern Arctic glacier marginal zones, Petuniabukta, Spitsbergen, Pol. Polar Res., 26, 239–258, 2005.

Hagen, J. O., Liestøl, O., Roland, E., and Jørgensen, T.: Glacier Atlas of Svalbard and Jan Mayen, Norwegian Polar Institute, Oslo, 1993.

Hagen, J. O., Kohler, J., Melvold, K., and Winther, J.-G.: Glaciers in Svalbard: mass balance, runoff and freshwater flux, Polar Res., 22, 145–159, 2003.

Hodgkins, R., Hagen, J. O., and Hamran, S.-E.: 20th century mass balance and thermal regime change at Scott Turnerbreen, Svalbard, Ann. Glaciol., 28, 216–220, 1999.

IPCC: Climate Change 2013, The Physical Science Basis, Working Group I Contribution to the Fifth Assessment Report of the Intergovernmental Panel on Climate Change, WMO/UNEP, Cambridge University Press, Geneva, 2013.

James, T. D., Murray, T., Barrand, N. E., Sykes, H. J., Fox, A. J., and King, M. A.: Observations of enhanced thinning in the upper reaches of Svalbard glaciers, The Cryosphere, 6, 1369–1381, doi:10.5194/tc-6-1369-2012, 2012.

Karczewski, A.: The development of the marginal zone of the Hørbyebreen, Petuniabukta, central Spitsbergen, Pol. Polar Res., 10, 371–377, 1989.

Kohler, J., James, T. D., Murray, T., Nuth, C., Brandt, O., Barrand, N. E., Aas, H. F., and Luckman, A.: Acceleration in thinning rate on western Svalbard glaciers, Geophys. Res. Lett., 34, L18502, doi:10.1029/2007GL030681, 2007.

König, M., Nuth, C., Kohler, J., Moholdt, G., and Pettersen, R.: A digitial glacier database for Svalbard, in: Global Land Ice Measurements from Space, Springer Berlin Heidelberg, Ch. 10, 229–239, 2013.

Kostrzewski, A., Kaniecki, A., Kapuściński, J., Klimczak, R., Stach, A., and Zwoliński, Z.: The dynamics and rate of denudation of glaciated and non-glaciated catchments, central Spitsbergen, Pol. Polar Res., 10, 317–367, 1989.

Lankauf, K. R.: Recesja lodowców rejonu Kaffiøyry (Ziemia Oskara II - Spitsbergen) w XX wieku (Retreat of Kaffiøyra glaciers [Oscar II Land – Spitsbergen] in the 20th century), Prace Geograficzne nr. 183, Polska Akademia Nauk, Warszawa, 2002.

Láska, K., Witoszová, D., and Prošek, P.: Weather patterns of the coastal zone of Petuniabukta, central Spitsbergen in the period 2008–2010, Pol. Polar Res., 33, 297–318, 2012.

TCD
9, 6153–6185, 2015

Li, Y., and Li, Y.: Topographic and geometric controls on glacier changes in the central Tien Shan, China, since the Little Ice Age, Ann. Glaciol., 55, 177–186, 2014 doi:10.3189/2014AoG66A031, 2014.

Lid, J.: Mariskardet på Svalbard, Norsk Geogr. Tidsskr., 2, 445–460, 1928.

Lovell, H., Fleming, E. J., Benn, D. I., Hubbard, B., Lukas, S., and Naegeli, K.: Former dynamic behaviour of a cold-based valley glacier on Svalbard revealed by basal ice and structural glaciology investigations, J. Glaciol., 61, 309–328, 2015.

Małecki, J.: The Present-Day State of Svenbreen (Svalbard) and Changes of its Physical Properties After the Termination of the Little Ice Age, PhD thesis, Adam Mickiewicz University in Poznań, Poland, 145 pp., 2013a.

Małecki, J.: Elevation and volume changes of seven Dickson Land glaciers, Svalbard, Polar Res., 32, 18400, 2013b.

Małecki, J.: Some comments on the flow velocity and thinning of Svenbreen, Dickson Land, Svalbard, Czech Polar Reports, 4, 1–8, 2014.

Małecki, J.: Glacio-meteorology of Ebbabreen, Dickson Land, central Svalbard, during 2008–2010 melt seasons, Pol. Polar Res., 36, 145–161, 2015a.

Małecki, J.: Snow accumulation on a small high-Arctic glacier Svenbreen – variability and topographic controls, Geogr. Ann. A., in press, 2015b.

Małecki, J., Faucherre, S., and Strzelecki, M.: Post-surge geometry and thermal structure of Hørbyebreen, central Spitsbergen, Pol. Polar Res., 34, 305–321, 2013.

Martín-Español, A., Navarro, F. J., Otero, J., Lapazaran, J. J., and Błaszczyk, M.: Estimate of the total volume of Svalbard glaciers, and their potential contribution to sea-level rise, using new regionally based scaling relationships, J. Glaciol., 61, 29–41, doi:10.3189/2015JoG14J159, 2015.

Moholdt, G., Nuth, C., Hagen, J. O., and Kohler, J.: Recent elevation changes of Svalbard glaciers derived from ICESat laser altimetry, Remote Sens. Environ., 114, 2756–2767, 2010.

Nordli, Ø., Przybylak, R., Ogilvie, A. E. J., and Isaksen, K.: Long-term temperature trends and variability on Spitsbergen: the extended Svalbard Airport temperature series, 1898–2012, Polar Res., 33, 21348, doi:10.3402/polar.v33.21349, 2014.

Norwegian Polar Institute: Terrengmodell Svalbard (S0 Terrengmodell), Norwegian Polar Institute, Tromsø, Norway, available at: https://data.npolar.no/dataset/dce53a47-c726-4845-85c3-a65b46fe2fea, last access: 3 March 2015, 2014a.

Norwegian Polar Institute: Kartdata Svalbard 1 : 100 000 (S100 Kartdata), Norwegian Polar Institute, Tromsø, Norway, avaliable at: https://data.npolar.no/dataset/645336c7-adfe-4d5a-978d-9426fe788ee3, last access: 2 January 2015, 2014b.

Nuth, C. and Kääb, A.: Co-registration and bias corrections of satellite elevation data sets for quantifying glacier thickness change, The Cryosphere, 5, 271–290, doi:10.5194/tc-5-271-2011, 2011.

Nuth, C., Kohler, J., Aas, H. F., Brandt, O., and Hagen, J. O.: Glacier geometry and elevation changes on Svalbard (1936–90): a baseline dataset, Ann. Glaciol., 46, 106–116, 2007.

Nuth, C., Moholdt, G., Kohler, J., Hagen, J. O., and Kääb, A.: Svalbard glacier elevation changes and contribution to sea level rise, J. Geophys. Res., 115, F01008, doi:10.1029/2008JF001223, 2010.

Nuth, C., Kohler, J., König, M., von Deschwanden, A., Hagen, J. O., Kääb, A., Moholdt, G., and Pettersson, R.: Decadal changes from a multi-temporal glacier inventory of Svalbard, The Cryosphere, 7, 1603–1621, doi:10.5194/tc-7-1603-2013, 2013.

Oerlemans, J.: Extracting a climate signal from 169 glacier records, Science, 308, 675–677, doi:10.1126/science.1107046, 2005.

Paul, F. and Mölg, N.: Hasty retreat of glaciers in northern Patagonia from 1985 to 2011, J. Glaciol., 60, 2014, doi:10.3189/2014JoG14J104, 2014.

Pleskot, K.: Sedimentological characteristics of debris flow deposits within ice-cored moraine of Ebbabreen, central Spitsbergen, Pol. Polar Res., 36, 125–144, 2015.

Pohjola, V. A., Martma, T., Meijer, H. A. J., Moore, J. C., Isaksson, E., Vaikmae, R., and van de Wal, R. S. W.: Reconstruction of three centuries of annual accumulation rates based on the record of stable isotopes of water from Lomonosovfonna, Svalbard, Ann. Glaciol., 35, 57–62, 2002.

Przybylak, R., Araźny, A., Nordli, Ø., Finkelnburg, R, Kejna, M., Budzik, T., Migała, K., Sikora, S., Puczko, D., Rymer, K., and Rachlewicz, G.: Spatial distribution of air temperature on Svalbard during 1 year with campaign measurements, Int. J. Climatol., 34, 3702–3719, 2014, doi:10.1002/joc.3937, 2014.

Rachlewicz, G.: Contemporary Sediment Fluxes and Relief Changes in High Arctic Glacierized Valley Systems (Billefjorden, Central Spitsbergen), Uniwersytet im, Adama Mickiewicza w Poznaniu, seria geografia nr 87, Wydawnictwo Naukowe UAM, Poznań, Poland, 2009a.

Rachlewicz, G.: River floods in glacier-covered catchments of the high Arctic: Billefjorden-Wijdefjorden, Svalbard, Norsk Geogr. Tidsskr., 63, 115–122, 2009b.

Rachlewicz, G. and Styszyńska, A.: Porównanie przebiegu temperatury powietrza w Petuniabukta i Svalbard-Lufthavn (Isfjord, Spitsbergen) w latach 2001–2003 (Comparison of the course of air temperature in Petuniabukta and Svalbard-Lufthavn (Isfjord, Spitsbergen) in the years 2001–2003), Problemy Klimatologii Polarnej, 17, 121–134, 2007.
Rachlewicz, G., Szczuciński, W., and Ewertowski, M.: Post-"Little Ice Age" retreat rates of glaciers around Billefjorden in central Spitsbergen, Svalbard, Pol. Polar Res., 28, 159–186, 2007.
Radić, V. and Hock, R.: Regionally differentiated contribution of mountain glaciers and ice caps to future sea-level rise, Nat. Geosci., 4, 91–94, 2011.
Sobota, I.: Selected methods in mass balance estimation of Waldemar Glacier, Spitsbergen, Pol. Polar Res., 28, 249–268, 2007.
Strzelecki, M. C., Małecki, J., Zagórski, P.: The influence of recent deglaciation and associated sediment flux on the functioning of polar coastal zone – northern Petuniabukta, Svalbard, in: Sediment Fluxes in Coastal Areas, Coastal Research Library 10, edited by: Maanan, M. and Robin, M., Springer Science + Business Media, Dordrecht, 23–45, ISBN 978-94-017-9259-2, 2014.
Szpikowski, J., Szpikowska, G., Zwoliński, Z., Rachlewicz, G., Kostrzewski, A., Marciniak, M., and Dragon, K.: Character and rate of denudation in a High Arctic glacierized catchment (Ebbaelva, Central Spitsbergen), Geomorphology, 218, 52–62, doi:10.1016/j.geomorph.2014.01.012, 2014.
Troicki, L. S.: O balanse massy lednikov raznyh typov na Špicbergenie (On the mass balance of different types of glaciers on Spitsbergen), Materialy Glyaciologičeskih Issledovanij, 63, 117–121, 1988.
Wouters, B., Chambers, D., and Schrama, E. J. O.: GRACE observes small-scale mass loss in Greenland, Geophys. Res. Lett., 35, L20501, doi:10.1029/2008GL034816, 2008.
Zagórski, P., Siwek, K., Gluza, A., and Bartoszewski, S. A.: Changes in the extent and geometry of the Scott Glacier, Spitsbergen, Pol. Polar Res., 29, 163–185, 2008.
Ziaja, W.: Glacial recession in Sørkappland and central Nordenskiöldland, Spitsbergen, Svalbard, during the 20th century, Arct. Antarct. Alp. Res., 33, 36–41, 2001.
Žuravlev, A. B., Mačeret, J. J., and Bobrova, L. I.: Radiolokalicjonnije issledovanije na poljarnom lednike s zimnym stokom (Radio-echo sounding investigations on a polar glacier with winter discharge), Materialy Glyaciologičeskih Issledovanij, 46, 143–149, 1983.

TCD
9, 6153–6185, 2015

Strong ELA increase causes fast mass loss of glaciers, Spitsbergen

J. Małecki

Table 1. Changing extent of glaciers in Dickson Land in the study periods.

Subregion	Area, A (km^2) Max	1960's	1990	2009/11	Area change, dA Max–2009/11	Length change rates, dL/dt ($m\,a^{-1}$) Max–1960's	1960's–1990	1990–2009/11	Max–2009/11
DL-N	91.76 ± 12.03	78.65 ± 3.35	63.83 ± 2.74	51.05 ± 1.43	−44.4 ± 14.4 %	−6.6 ± 0.2	−10.0 ± 0.2	−19.7 ± 0.1	−9.8 ± 0.1
DL-C	174.95 ± 18.14	159.55 ± 11.81	137.88 ± 4.10	117.07 ± 2.22	−33.1 ± 11.0 %	−4.7 ± 0.2	−10.1 ± 0.2	−18.1 ± 0.1	−8.4 ± 0.1
DL-S	67.40 ± 8.25	63.98 ± 4.17	50.27 ± 1.71	39.32 ± 0.92	−41.7 ± 13.3 %	−3.6 ± 0.2	−7.0 ± 0.3	−11.4 ± 0.1	−6.1 ± 0.1
Total	334.11 ± 38.42	302.18 ± 19.34	251.98 ± 8.57	207.44 ± 4.56	−37.9 ± 12.1 %	−5.1 ± 0.1	−9.4 ± 0.1	−17.2 ± 0.1	−8.4 ± 0.1

TCD
9, 6153–6185, 2015

Strong ELA increase causes fast mass loss of glaciers, Spitsbergen

J. Małecki

TCD
9, 6153–6185, 2015

Strong ELA increase causes fast mass loss of glaciers, Spitsbergen

J. Małecki

Table 2. Elevation changes, volume changes and mass balance of glaciers in subregions of Dickson Land over the period 1990–2011.

Subregion	Volume and elevation changes, d*V* and d*H*, and their rates d*V*/d*t* and d*H*/d*t*				
	d*V* (millions m^3)	d*V*/d*t* (millions $m^3\,a^{-1}$)	d*H* (m)	d*H*/d*t* ($m\,a^{-1}$)	Mass balance (m w.e.)
DL-N	−735 ±46	−35.0 ±2.3	−12.8 ±1.1	−0.61 ±0.05	−0.55 ±0.04
DL-C (total)	−1987 ±256	−94.6 ±12.5	−15.6 ±2.2	−0.74 ±0.11	−0.67 ±0.10
DL-C Surveyed	−1482 ±67	−70.6 ±3.3	−16.6 ±1.2	−0.79 ±0.06	−0.71 ±0.07
DL-C Unsurveyed*	−505 ±247	−24.0 ±12.0	−13.1 ±6.6	−0.63 ±0.32	−0.56 ±0.28
DL-S	−651 ±37	− 31.0 ±1.8	−14.5 ±1.2	−0.69 ±0.06	−0.62 ±0.05
Total	−3372 ±273	−160.6 ±13.0	−14.7 ±1.2	−0.70 ±0.06	−0.63 ±0.05

* estimates based on the relationship between d*H*/d*t* and tELA.

Table 3. Pearson correlation coefficients for glacier change indicators against other indicators and geometry parameters. Bold values indicate statistical significance at $p = 0.01$ level.

	dA Max–2009/11	dA 1990–2009/11	dL/dt Max–2009/11	dL/dt 1990–2009/11	Relative dL Max–2009/11	Relative dL 1990–2009/11	dH/dt	ln(A_{max})	ln(A_{2011})	L_{max}
dA Max–2009/11	1	**0.40**	0.19	0.16	**0.79**	**0.59**	**0.21**	**0.42**	**0.60**	**0.49**
dA 1990–2009/11	**0.40**	1	−0.15	0.16	**0.44**	**0.59**	0.08	**0.33**	**0.50**	**0.50**
dL/dt Max–2009/11	0.19	−0.15	1	**0.69**	**0.54**	**0.35**	0.11	**−0.43**	**−0.33**	**−0.59**
dL/dt 1990–2009/11	0.16	0.16	**0.69**	1	**0.41**	**0.70**	**0.37**	**−0.35**	−0.28	**−0.43**
Relative dL Max–2009/11	**0.79**	**0.44**	**0.54**	**0.41**	1	**0.78**	0.19	**0.37**	**0.57**	0.18
Relative dL 1990–2009/11	**0.59**	**0.59**	**0.35**	**0.70**	**0.78**	1	**0.37**	0.26	**0.46**	0.18
dH/dt	**0.21**	0.08	0.11	**0.37**	0.19	**0.37**	1	**−0.48**	**−0.33**	−0.02

Discussion Paper | Discussion Paper | Discussion Paper | Discussion Paper |

TCD
9, 6153–6185, 2015

Strong ELA increase causes fast mass loss of glaciers, Spitsbergen

J. Małecki

Title Page
Abstract | Introduction
Conclusions | References
Tables | Figures
◂◂ | ▸▸
◂ | ▸
Back | Close
Full Screen / Esc
Printer-friendly Version
Interactive Discussion

Table 3. Continued.

	L_{2011}	H_{med}	H_{min}	H_{max}	H_{mor}	tELA	S	$\cos\alpha$	Longitude	Latitude
dA Max–2009/11	**0.64**	**0.24**	−0.12	**0.51**	0.03	**0.21**	**−0.31**	−0.11	0.14	**0.24**
dA 1990–2009/11	**0.53**	0.13	−0.16	**0.38**	−0.08	0.10	**−0.27**	0.03	0.09	**0.23**
dL/dt Max–2009/11	**−0.32**	0.19	**0.53**	−0.22	**0.73**	0.23	0.08	0.11	−0.05	−0.09
dL/dt 1990–2009/11	−0.25	0.20	**0.43**	−0.14	**0.46**	0.21	0.08	−0.03	−0.08	−0.03
Relative dL Max–2009/11	**0.41**	0.22	−0.20	**0.35**	0.23	0.18	**−0.62**	−0.19	0.16	0.28
Relative dL 1990–2009/11	**0.35**	0.11	−0.24	0.26	0.07	0.06	**−0.50**	−0.23	0.04	0.20
dH/dt	0.02	**0.72**	**0.69**	**0.31**	**0.67**	**0.74**	**0.41**	0.02	0.00	**0.25**

TCD
9, 6153–6185, 2015

Strong ELA increase causes fast mass loss of glaciers, Spitsbergen

J. Małecki

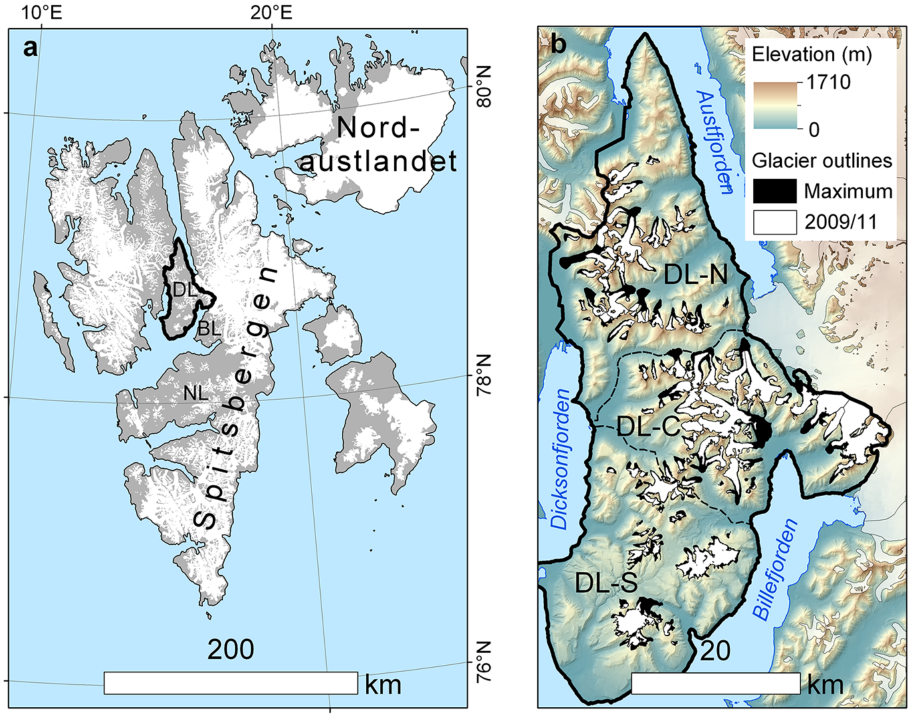

Figure 1. Location of the study area. **(a)** Map of Svalbard with location of regions of central Spitsbergen: Dickson Land (DL), Nordenskiöld Land (NL) and Bünsow Land (BL); **(b)** map of Dickson Land and its subregions: north (DL-N), central (DL-C) and south (DL-S).

TCD
9, 6153–6185, 2015

Strong ELA increase causes fast mass loss of glaciers, Spitsbergen

J. Małecki

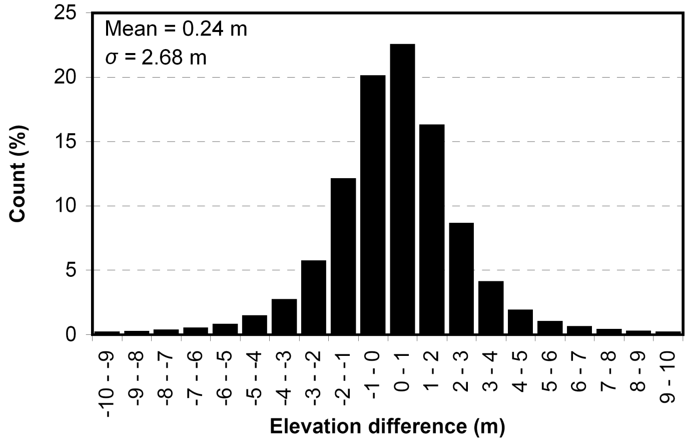

Figure 2. Histogram of elevation differences between 2009/11 DEM and 1990 DEM over non glacier-covered terrain.

TCD
9, 6153–6185, 2015

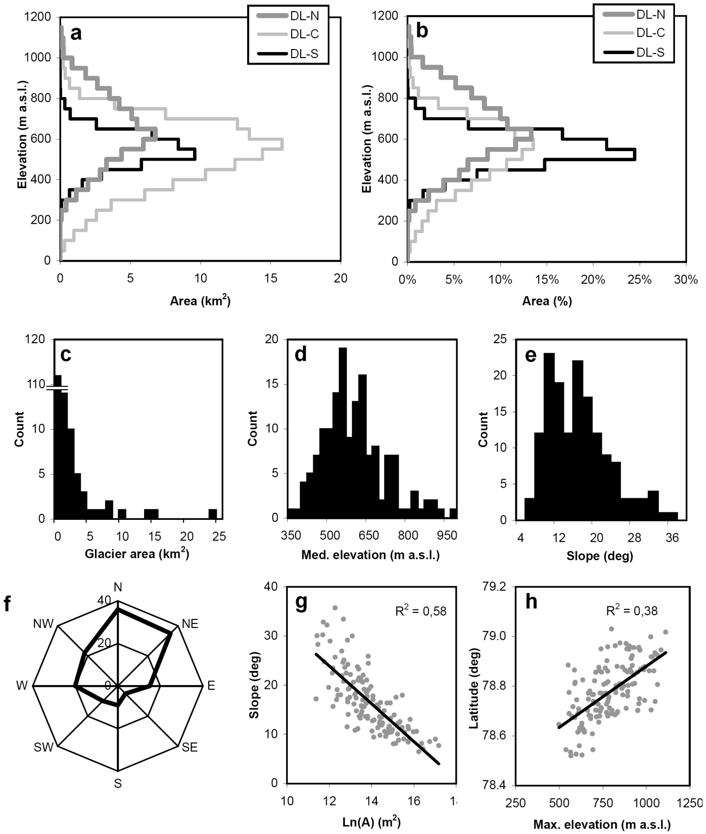

Figure 3. Glacier geometry in Dickson Land in 2009/11. Altitude of ice cover in subregions of Dickson Land against absolute area **(a)** and relative area ice cover **(b)**. Frequency distribution of glacier areas **(c)**, median elevations **(d)**, slopes **(e)** and mean aspects **(f)**, scatter plot of glacier slopes against ln(area) **(g)** and scatter plot of latitude against maximum glacier elevations **(h)**.

TCD
9, 6153–6185, 2015

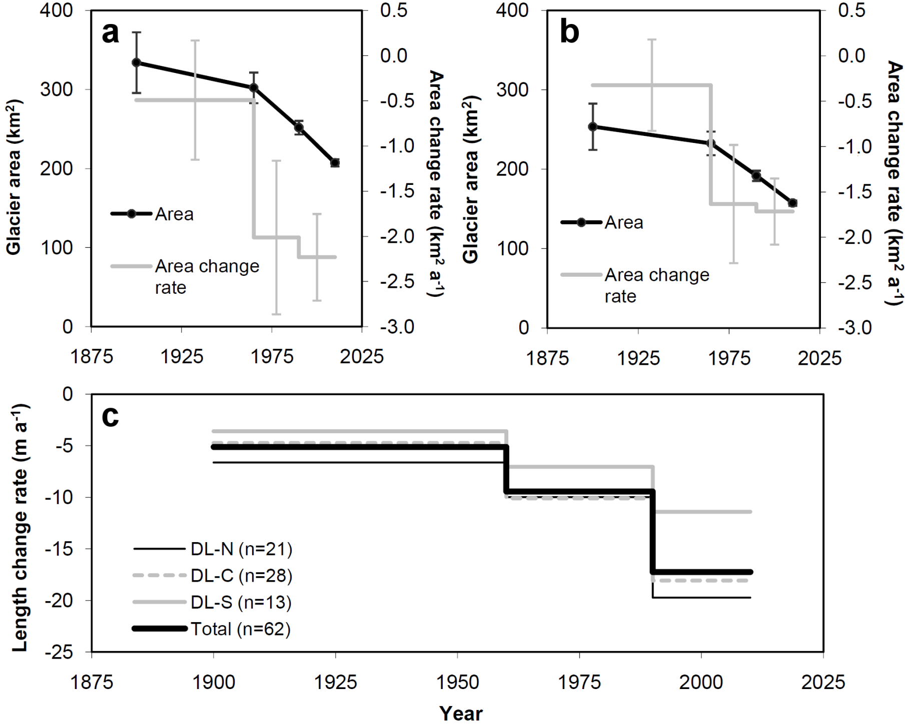

Figure 4. Total Dickson Land glacier area changes and area change rates for all glaciers **(a)** and non-surging glaciers only **(b)** and average glacier length change rates in Dickson Land and its subregions: north (DL-N), central (DL-C) and south (DL-S).

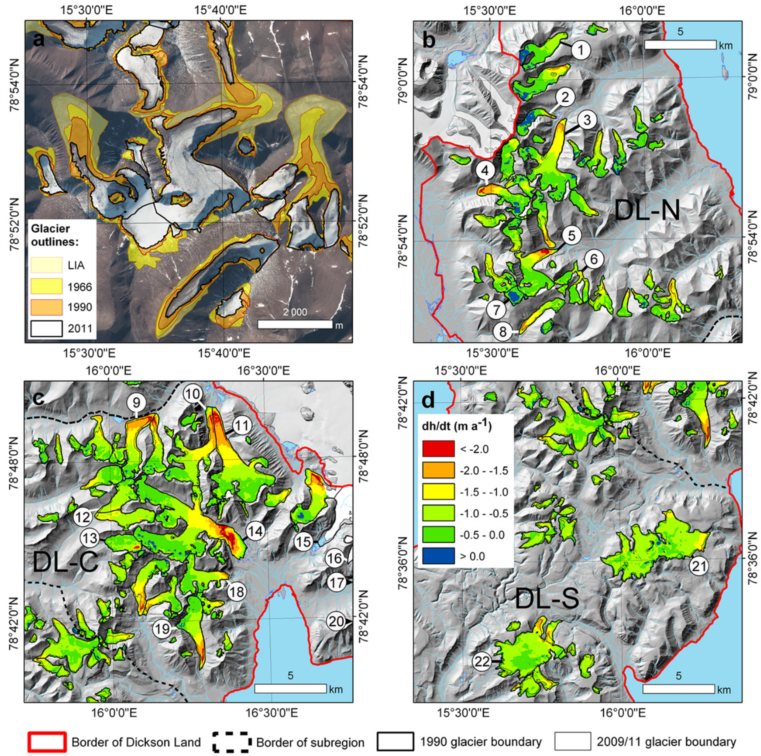

Figure 5. An example of glacier area changes in northern Dickson Land in Delbreen region **(a)** and mean 1990–2009/11 elevation change rates in northern **(b)**, central **(c)** and southern **(d)** Dickson Land with location of glaciers mentioned in the text: 1 – Kaalaasbreen, 2 – Arbobreen, 3 – Hoegdalsbreen, 4 – Fyrisbreen, 5 – Vasskilbreen, 6 – Delbreen, 7 – Gavlhaugen ice patch, 8 – Sophusbreen, 9 – Manchesterbreen, 10 – Baliolbreen, 11 – Cambridgebreen, 12 – Gonvillebreen, 13 – Stensiobreen, 14 – Hørbyebreen, 15 – Ragnarbreen, 16 – Bertrambreen, 17 – Ebbabreen, 18 – Svenbreen, 19 – Bertilbreen, 20 – Pollockbreen, 21 – Jotunfonna, 22 – Frostisen. Base map for **(a)**: ©Norwegian Polar Institute.

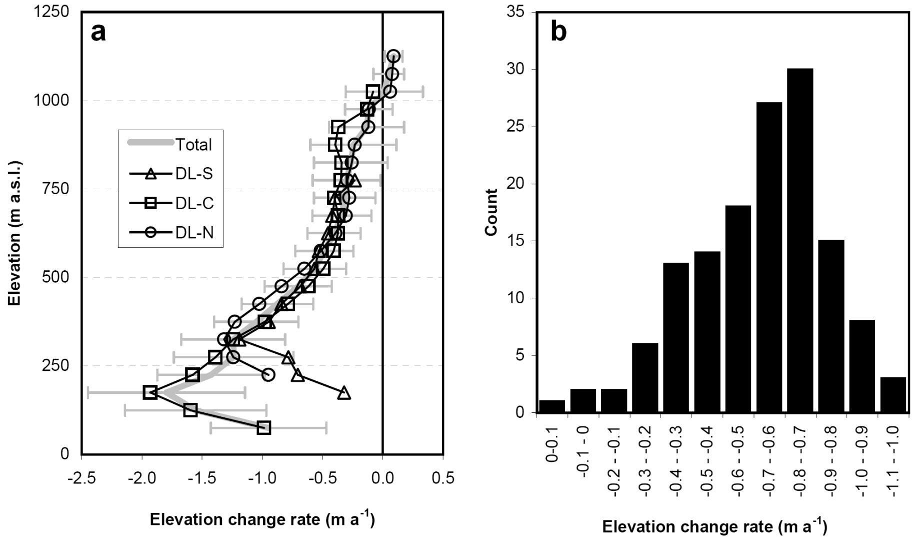

Figure 6. Glacier thinning in Dickson Land over the period 1990–2009/11: **(a)** average elevation change curves for Dickson Land (with one standard deviation bars) and its subregions and **(b)** frequency distribution of geodetic balances.

TCD
9, 6153–6185, 2015

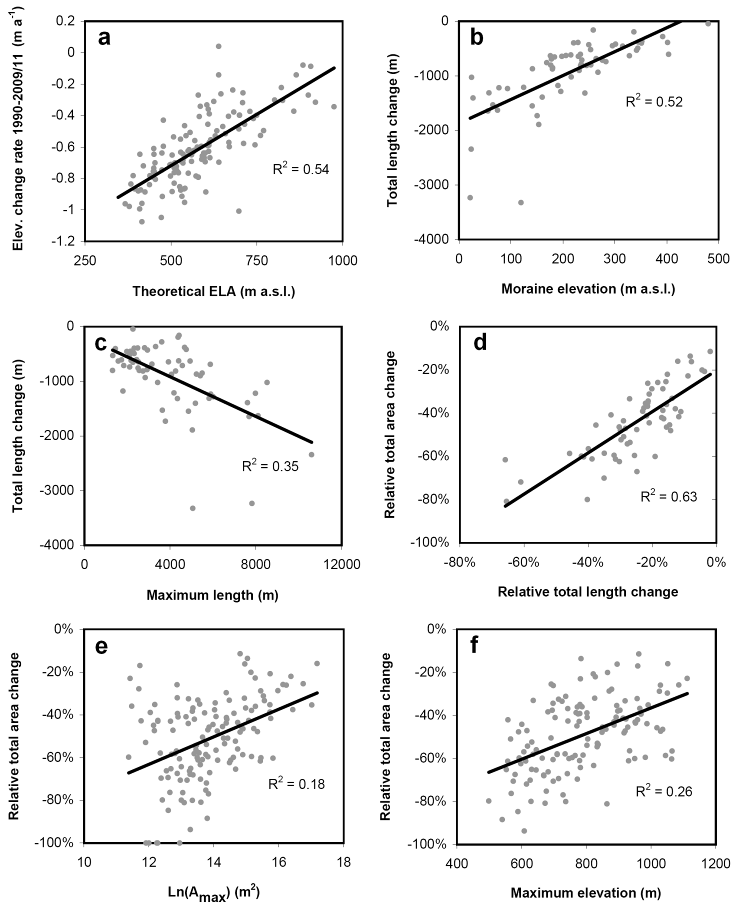

Figure 7. Scatter plots of selected glacier change indicators against geometry parameters or other indicators.

TCD

9, 6153–6185, 2015